ELSEVIER

Contents lists available at ScienceDirect

BBA Advances

journal homepage: www.sciencedirect.com/journal/bba-advances





Membrane dynamics are slowed for Alexa594-labeled membrane proteins due to substrate interactions

Alan W. Weisgerber, Michelle K. Knowles

Department of Chemistry and Biochemistry, University of Denver, Denver, CO 80210, USA

ABSTRACT

The addition of fluorescent dyes to proteins, lipids and other biological molecules can affect a range of processes such as mobility, molecular interactions, localization, and, ultimately, function. The dynamics of a protein can be dramatically affected if the label interacts non-specifically with the substrate or with other molecules in the system. To test how dye-substrate interactions affect protein diffusion, fluorescence recovery after photobleaching (FRAP) measurements were designed to explicitly determine the role of the dye on the diffusion of a transmembrane protein, Syntaxin1a, expressed on the cell surface. Syntaxin1a, was tagged with EGFP on the extracellular side and an EGFP nanobody with or without a dye label was attached. FRAP was performed on Syx1a-EGFP and the choice of cell growth substrate affected mobility in the presence of a dye labeled nanobody. This work provides evidence for choosing fibronectin (Fn) over poly-L-lysine (PLL) in FRAP and single molecule tracking measurements when using Alexa594, a common probe for red fluorescent measurements. Alexa594-labeled nanobody but not unlabeled nanobody, dramatically reduced the mobility of Syx1a-EGFP when cells were cultured on PLL. However, when Fn was used, the mobility returned. Mobility measured by single molecule tracking measurements align with the FRAP measurements with Fn coated surfaces being more mobile than PLL.

1. Introduction

Recent advancements in imaging methods that probe protein mobility rely on the use of organic fluorescent dyes [1, 2], which are notably brighter and more photostable for imaging measurements. Therefore, organic dyes are widely used in single molecule tracking, super-resolution and fluorescence recovery after photobleaching (FRAP) experiments to study the localization, mobility and dynamics of proteins [2-4]. Fluorescent labels for cellular imaging are ideally designed when there is minimal interaction with the system; probes should be unbiased reporters for the location of a protein of interest. Therefore, probes need to avoid: 1) membrane insertion, 2) multimerization/aggregation, and 3) non-specific, substrate binding. These types of interactions will affect the measurement of membrane protein dynamics, typically leading to a reduction in the mobility of the protein studied.

There is clear evidence that commonly used dyes have unintended interactions with membranes, causing mobility to be hindered due to non-physiological artifacts. For example, lipid mixing kinetics are affected by the probe choice in viral fusion assays, with the dye R18 mixing at a lower efficiency than TexasRed [5]. Dyes interact and insert into membranes depending on the dye and membrane physico-chemical characteristics. In a large scale screen of 32 dyes for dye-membrane interactions, it was determined that that highly charged dyes have lower membrane interaction factors when compared to uncharged or

singly charged dyes and, typically, larger dyes (red dyes) interact more with membranes [6]. In all-atom molecular dynamics simulations of dyes (Cy3, Cy5) with membranes the insertion of dyes into the membrane was initiated by a charge interaction between the lipid headgroup and the dye, followed by a slower insertion of the hydrophobic portion of the dye into the membrane [3]. To alleviate issues, dyes often contain charges to minimize non-specific interactions with cell membranes.

Multimerization has been an issue for a variety of probes, such as organic dyes attached to antibodies and fluorescent proteins [7, 8]. Multimerization can lead altered dynamics as membrane proteins have a larger drag through the membrane [9]. To combat this, dye labeled nanobodies, which are monovalent, single domain antibodies, have been a valid strategy for reducing the effects of multivalent binding observed with traditional antibodies [10]. The popularity of nanobodies as labeling entities for membrane proteins has grown over the past 10 years, with the design of nanobodies that recognize specific protein conformations [11] and ones that bind specifically to GFP [12]. In this work, a nanobody that binds EGFP on the surface of cells was purified, dye-labeled, and added to cells in culture prior to imaging.

A third interaction known to affect protein dynamics is that of the dye with the cell growth substrate. Recent work shows that different organic dyes adhere differentially to a variety of surface coatings [13, 14] and this interaction is likely due to the hydrophobicity of the dye, with hydrophilic dyes resulting in fewer non-specific bindings compared

^{*} Corresponding author at: Department of Chemistry and Biochemistry, University of Denver, Denver, CO 80210, USA *E-mail address*: michelle.knowles@du.edu (M.K. Knowles).

to hydrophobic dyes, which were correlated to lower mobility and higher instances of non-specific binding [13]. To assess cell growth substrate binding, immobility of a variety of dye-affibody conjugations with different targets were measured. The conclusion was that there were many factors to dye interactions were challenging to predict accurately, since substrate, dye selected, and protein of interest all play crucial roles [13]. As a result, all three materials should be tested and specifically chosen for the experiment.

Cell growth substrates vary widely in their overall charge, method of cell attachment and their ability to adhere to glass surfaces used in microscopy. In this work, poly-L-lysine (PLL) and fibronectin (Fn) were used. PLL is a polypeptide consisting of lysine amino acids, making PLL a positively charged substrate. Cells attach via nonspecific electrostatic interactions with the negatively charged cell membrane [15]. Fn is a glycoprotein that interacts with integrin receptors to facilitate cell attachment and spreading [15-17]. Fn is negatively charged (pI 5.5–6.0) and has a hydrophobic binding domain for cell attachment. Many dyes carry a negative charge to prevent insertion and interactions with cell membranes, potentially leading to non-specific binding to cell substrates [13, 14]. In this work, Alexa594 was used and contains an overall -2 charge.

Elucidating probe interactions with the cell growth substrate is challenging to determine because comparison to a probe-free measurement cannot typically be made; a fluorescent marker must be used for imaging. In this work, we overcome this and describe a FRAP-based assay that can specifically measure how dyes affect mobility. In this assay, the mobility of an externally exposed eGFP attached to a transmembrane protein on the cell surface (Syntaxin1a-EGFP) was measured. The effects of a nanobody to EGFP, with and without a dye label, on membrane protein dynamics was determined. This differential type of measurement directly probes how the dye alters the dynamics. Several surface treatments were compared for their ability to non-specifically bind dyes. Alexa594-labeled nanobody but not unlabeled nanobody, dramatically reduced the mobility of Syx1a-EGFP. The dye's ability to affect mobility was identified to be due to an interaction with a commonly used substrate for cell adhesion, PLL. However, when Fn was used, the mobility returned. Single molecule tracking measurements align with the FRAP measurements with Fn coated surfaces being more mobile than PLL. Overall, we observed dye and surface coating dependent interactions that affected membrane protein dynamics and were able to alleviate this by using Fn.

2. Materials and methods

All buffer reagents were purchased from Sigma Aldrich except when noted.

Substrate Coating: Coverglass (Ted Pella, 25mm round, #1.5 thickness) was coated with poly-L-lysine ("PLL", Sigma Aldrich, P4707) and/ or fibronectin ("Fn", Gibco, 33016015). For PLL coating, glass was cleaned by soaking overnight in 0.1% bleach solution, followed by rinsing thoroughly in DI water. PLL was added to the coverglass and incubated at room temperature for 15 minutes then rinsed three times with DPBS containing Ca²⁺ and Mg²⁺(Gibco). For Fn coated glass, several approaches were taken. A 3M solution of potassium hydroxide was used to etch glass following the methods described previously [18]. Coverglass was also taken straight from the package, dipped in ethanol and flamed for approximately 5 seconds, then coated with Fn. Results from both methods were similar, but flame treating is simpler to do. Fn was also coated to PLL coated coverslips, where PLL was applied as described above then Fn was incubated for 15 minutes or overnight. The concentration of Fn ranged from 2 $\mu g/ml$ to 50 $\mu g/ml$ and noted in the figure captions.

Cell Culture: PC12-GR5 cells were grown as described previously [19]. Briefly, cells were maintained on T25 flasks (Life Science Products, Frederick, Colorado) in 10% CO₂ and 37° C. Cells were passaged up to 40 times before thawing a new batch of cells. Transfection was performed

with Lipofectamine 3000 (Thermo Fisher Scientific) according to manufacturer protocols but the amount DNA and Lipofectamine was reduced by half the recommendation to minimize cell damage. At 20-40 hours post-transfection cells were imaged in Imaging Buffer (140mM NaCl, 3mM KCl, 1mM MgCl₂, 3mM CaCl₂, 10mM D-Glucose, 10mM HEPES, pH 7.4). DNA plasmids Syx1a-eGFP-dCMV and Syx1a-eGFP were supplied from Wolfhard Almers [19, 20]. The dCMV promoter is a truncated promoter that dramatically reduces expression to be equivalent to the endogenous amount [19, 20]. This construct has been deposited at Addgene (#34631).

Nanobody Purification: BL21 cells were transformed with DNA expressing an anti-EGFP nanobody (Addgene, #49172) at 37°C in a 10 mL overnight starter culture with 2000x ampicillin 100 mg/mL. Starter cultures were then used to inoculate 1 L of Luria Broth (Alpha Bio-Sciences, Baltimore, MD, L12-112) and grown until OD600 of 0.9 after which induction started with 1 mL 1M IPTG (GoldBio, St. Louis, MO) and temperature was changed from 37°C to 20°C. Cells were allowed to express for 24 hours after which they were spun down at 6000xg for 15 min at 4°C. Cells were then frozen at -80°C until purification occurred. Cells were thawed on ice and resuspended in 20 mL Lysis Buffer (300mM NaCl, 50mM Na₃PO₄, 5mM Imidazole, pH 8.0). Lysozyme was added for a final concentration of 1 mg/mL and incubated on ice for 30 minutes. Cells were then sonicated for 2 minutes on ice and centrifuged at 14,000 rpm using a F14-14 \times 50cy rotor for 15 minutes at 4 $^{\circ}$ C. Supernatant was then filtered with a $0.22 \mu m$ syringe filter and run on the FPLC with a HisTrap HP column. Purified protein was dialyzed into 0.1M Sodium Bicarbonate Buffer (pH 8.3) for quantification and dye labeling.

Dye labeling: AlexaFluor594 NHS ester was purchased from Thermo Fisher Scientific (A20004). Nanobody (NB) was labeled according to the protocols from manufacturers. NB was purified and concentrated to 1 mg/ml then labeled and separated using an Amicon Ultra-4 Centrifugal Filter. Labeled NB (NB*) was aliquoted and stored for up to 12 months at 4° C. Once the labeling capacity of a NB* diminished, usually 2 months of use, a new aliquot was thawed.

Confocal Microscopy and Fluorescence Recovery After Photobleaching (FRAP): Cells transected for 24 - 48 hours were first blocked with 10% BSA in DMEM and incubated for 1 hr at 37°C. After incubation the BSA mixture was removed and a solution containing $0.325~\mu g/mL$ nanobody in Imaging Buffer was added and incubated for 15 minutes at 37°C.

The cells were washed three times with 2 mL of imaging buffer then imaged. A point-scanning confocal microscopy (Olympus Fluoview 3000) was used for FRAP measurements. A 16 pixel diameter (3.98 μm), circular region of interest containing Syx1a-eGFP was bleached using 488 nm excitation. Images were recorded at 2.17 seconds per frame while using both 488 nm and 561 nm lasers to image eGFP and Alexa594-NB*, respectively. FRAP data consisted of three frames prior to bleaching, followed by 3 seconds of bleaching and then observation of recovery for 100 frames. FRAP imaging took place at 20 - 22°C. The recovery was measured, corrected for photobleaching, and normalized against the average of the pre-photobleached frames, as described in our past work [21]. Graphpad Prism was used for all plotting, fitting and t-testing.

Total Internal Reflection Fluorescence Microscopy (TIRFM) and Single Particle Tracking: The cells, initially blocked with a 10% BSA enriched media, were incubated with 0.013 µg/mL dye conjugated nanobody in Imaging Buffer for a period of 15 minutes prior to washing. Imaging was performed as described here [22, 23]. Briefly, an inverted Nikon microscope equip with a 60x, 1.49 NA TIRFM objective and a 2.5x lens to further expand the image such that 1 pixel = 107 nm. A 491 nm laser and a 561 nm laser were used to excite eGFP and Alexa594 labeled NB, respectively. The fluorescence emission was detected after passing through a dichroic beam splitter (Chroma, Bellows Falls, VT) then into a Dual-View (Optical Insights, Exton, PA) that splits the fluorescence into a green and red channel. The green channel (emission filter, Chroma 525/50 nm) was used to identify cells transfected with Syx1a-eGFP and the red channel (emission filter, Chroma 605/75 nm) was used for

tracking Alexa594-NB*. The images were collected on an Andor iXon 897+ EMCCD with a gain of 300 at a rate of 20 Hz and MicroManager was used for image acquisition.

Syx1a-eGFP tracking was performed as described[19] using SPT methods are freely available for Matlab [24, 25]. Briefly, image sequences were bandpass filtered to remove high frequency, single pixel, noise and low frequency background noise. Spots were located based on a threshold and size, then tracking was performed to connect localizations from one frame to the next. The maximum distance a particle was allowed to travel between consecutive frames (50 ms) was 7 pixels, where one pixel is 107 nm. From the trajectories, the step size displacements were calculated with a time difference of 200 ms (4 frames). The step size displacement histograms were fit according to:

$$y(r,t) = r \left(A_1 \exp\left(-\frac{r^2}{4D_1 t}\right) + A_2 \exp\left(-\frac{r^2}{4D_2 t}\right) \right) \tag{1}$$

Where, r is the distance traveled, the step size, during the time t=200 ms. D_1 and D_2 are diffusion coefficients and A_1 and A_2 are amplitudes that are related to the fraction mobile and fraction immobile molecules here

3. Results

Alexa594 conjugated nanobody binds specifically to transfected cells. To determine if the Alexa594 conjugated anti-EGFP nanobody (Alexa594-NB*) specifically binds Syx1-EGFP, transfected cells were incubated with Alexa594-NB* and imaged using a confocal microscope (Fig. 1). Areas of the well that contained both transfected and nontransfected cells were specifically imaged to determine the specificity of the NB*-cell interaction; transfected cells retain red fluorescent NB*, but cells that are not transfected do not. A transfected cell (Fig. 1A) sits among a collection of untransfected cells as seen in the brightfield image (Fig 1C). Excitation of Alexa594 shows that the Alexa594-NB* conjugate selectively binds the Syx1A-EGFP expressing cell (Fig. 1B), but not the neighboring, non-transfected cells. Upon zooming into a region of the cell, the intensity of the NB* fluorescence overlaps with the intensity of

the Syx1a-eGFP fluorescence (Fig. 1D). An overlay of the cropped regions shows that clusters of Syx1a-EGFP are colocalized with the Alexa594-NB*. This visual conformation demonstrates that the nanobody conjugate is binding the target through the interaction depicted in Fig. 1E, and not adhering non-specifically to cells.

The mobility of Syx1a-GFP is hindered by the presence of Alexa594 labeled NB and PLL surface coatings. FRAP was performed on Syx1a-eGFP (Fig. 2) with no NB present, with unlabeled NB (NB) and with Alexa594-NB* (NB*) to determine if the NB or dye specifically affects the dynamics of Syx1a-eGFP. In all cases, the recovery of Syx1aeGFP was below 100%, however immobile molecules are expected. It is well established that Syx1a forms clusters on the surface of cells [20, 26-29] and these clusters are interchangeable with the surroundings [20], yet others observe that the mobile fraction between 0.6-0.7 [28]. In this work, Syx1a-EGFP recovered to 0.7 (Fig. 2C). However, the mobility of Syx1-EGFP decreased in the presence of Alexa594-NB* when cells were grown on PLL (Fig. 2). To determine if the loss of mobility was due to the dye or the NB, the mobility of Syx1-EGFP was measured in the presence of unlabeled NB and in the absence of NB. The results (Fig. 2C-D) showed similar mobility for Syx1-EGFP with unlabeled NB and without NB added. The fraction mobile was reduced from 0.69 to 0.52, approximately a 25% reduction. However, the rate of recovery (Fig. 2D) is not hindered; the molecules that are free are able to move normally. This suggests that the dye is interfering with the diffusion of Syx1-EGFP, creating an immobile portion.

The mobility of Syx1a-GFP is restored by changing the surface coating to Fn. To determine the cause of the decreased mobility with Alexa594-NB*, the glass surface coating was changed. If the reduction of mobility is due to an interaction with the cell membrane, then the change in surface coating should not recover the loss of mobility. However, if the loss of mobility was due to the dye interacting with the surface coating, the change in surface coating could improve mobility. The Alexa594 dye is negatively charged and PLL is positively charged, which suggests that a dye-substrate interaction is likely. Therefore, Fn was tested as a new growth substrate. Fn has an overall negative charge, with a pI below 6, but the application of Fn to glass surfaces is not

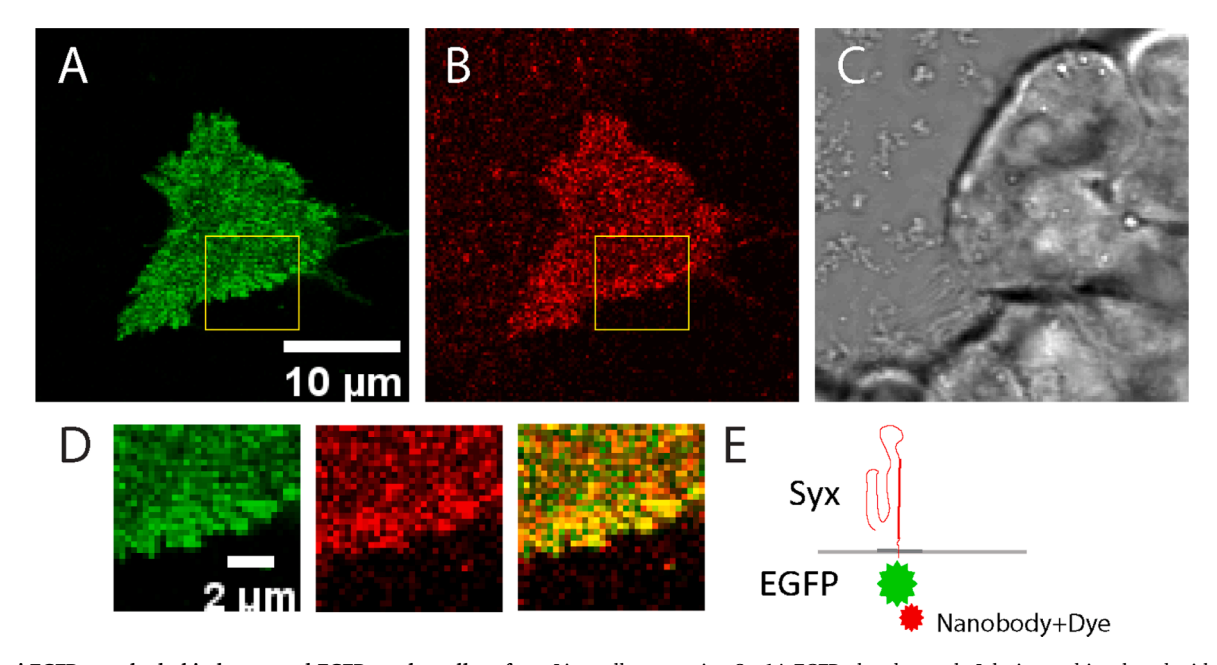


Fig. 1. Anti-EGFP nanobody binds exposed EGFP on the cell surface. Live cells expressing Syx1A-EGFP plated on poly-L-lysine and incubated with anti-EGFP nanobody conjugated to Alexa594 (Alexa594-NB*) were imaged by confocal microscopy 24 hours post-transfection. A) 488 nm excitation of the EGFP on the outside of the cell attached to Syx1A. B) Excitation of Alexa594-NB* with 561 nm. C) Brightfield image of all cells present. D) Clusters are observed in a cropped region from A (green) and B (red) and overlaid (yellow). E) A schematic of the labeling system used for dye-substrate investigations. Syx1a-eGFP is transiently expressed on the surface of PC12 cells with eGFP on the cell exterior. Anti-GFP NB with or without dye is added in subsequent experiments. (For the interpretation of the reference to the color in this figure legend. The reader is referred to the web version of this article)

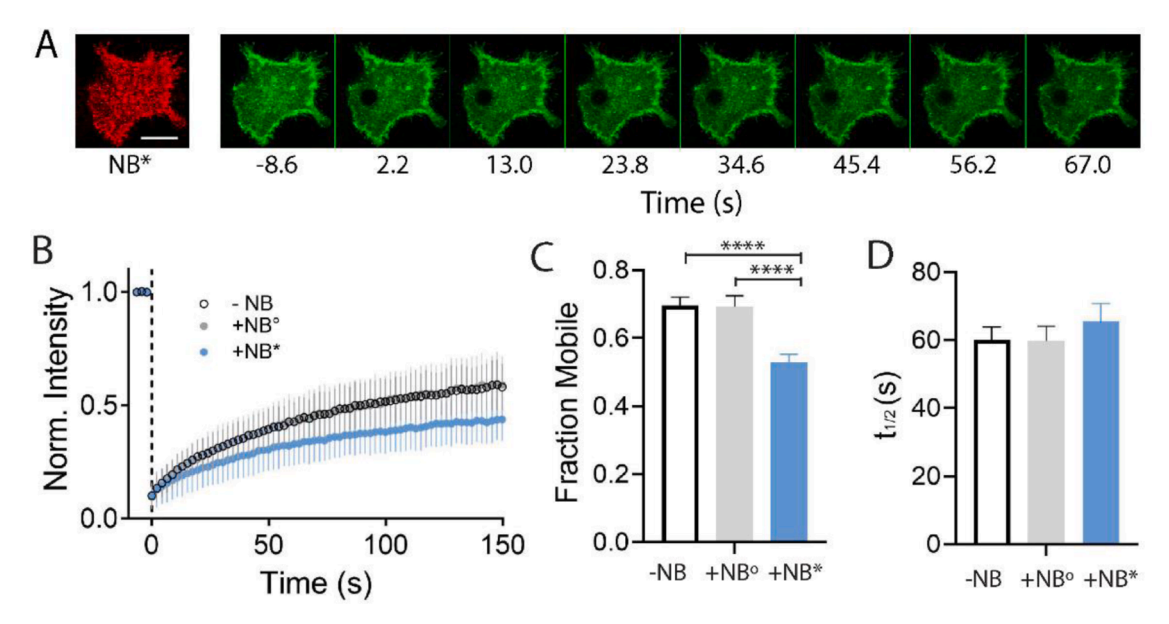


Fig. 2. Poly-L-Lysine coated glass surfaces restrict the motion of transmembrane proteins bound to Alexa594 labeled nanobody, but not unlabeled NB. Cells were plated on poly-L-lysine (PLL), transiently transfected with Syx1aEGFP, then imaged and photobleached on a confocal microscope. NB, if present, was incubated on cells for 15 m prior to imaging and rinsed twice in imaging buffer. A) A confocal image of Alexa594-NB* (red) and a montage with images separated by 10.8 s (5 frames) of the photobleaching of Syx1a-EGFP. Scale bar, $10 \mu m$. B) The FRAP recovery of Syx1a-EGFP with Alexa594-NB* present (+NB*, blue circles, N=18 cells), with unlabeled NB present (+NB°, grey circles, N=20 cells), and without NB present (-NB, empty circles, N=24 cells). C) The fraction mobile is reduced from 0.69 to 0.52 for samples with the dye present (p < 0.0001). D) The recovery rate, $t_{1/2}$, under the three conditions. Standard error is shown in all plots. (For the interpretation of the reference to the color in this figure legend. The reader is referred to the web version of this article)

straightforward. Coverglass was etched with 3M potassium hydroxide to facilitate adhesion of Fn to the glass surface. Afterwards, FRAP was measured with identical conditions to Fig. 2, with the exception that cells were grown on coverslips coated with Fn in place of PLL (Fig. 3). The results demonstrate that the mobility of Syx1A-EGFP with the NB-dye conjugate was similar to that of cells without any NB added (Fig. 3A-B). The fraction mobile was 0.71 and 0.70 for cells that

contained no NB (-NB) and Alexa594-NB* (NB*), respectively (Fig. 3C). The speed of the recovery, $t_{/2}$, was also similar for Syx-eGFP in the presence and absence of Alexa594-NB* (Fig. 3D). By changing the substrate to Fn, the restricted motion was fully recovered.

Fibronectin adheres well to KOH etched glass, but this treatment process requires a challenging preparation because concentrated KOH is not ideal to use due to its corrosive nature and strong vapors, therefore

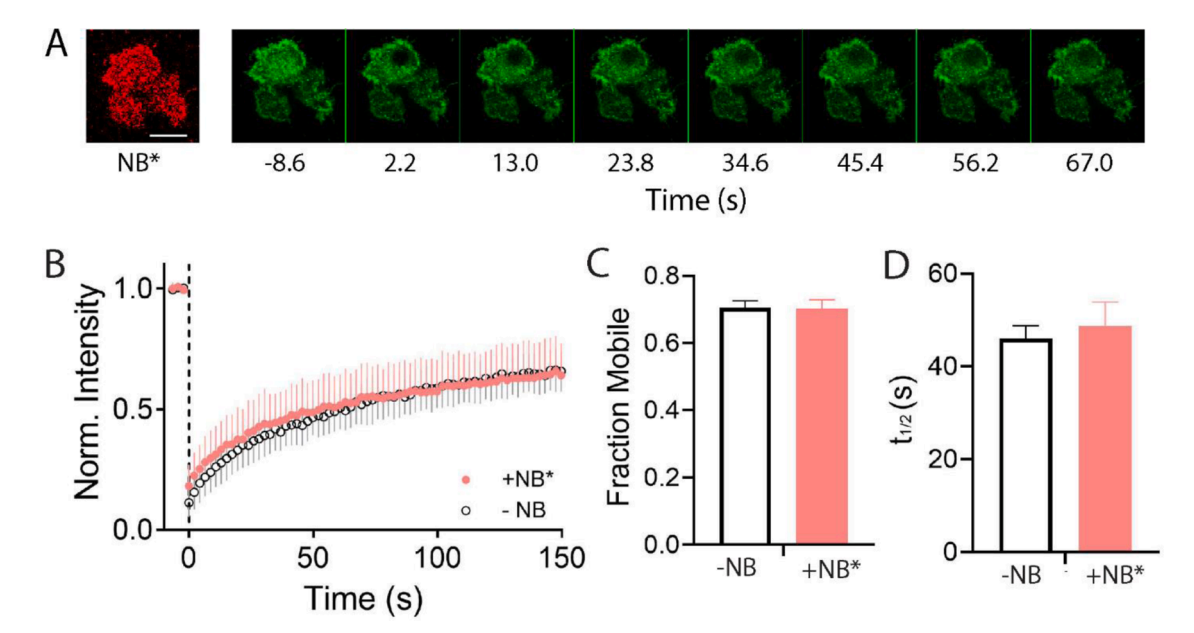


Fig. 3. Fibronectin coated KOH-etched glass does not impede the motion of transmembrane proteins containing Alexa594 labeled nanobody. Glass was treated with KOH then coated with fibronectin ($5 \mu g/ml$) and cells were plated then transiently transfected with Syx1a-EGFP. A) A confocal image of Alexa594-NB* (red) and a montage with images separated by 10.8 s (5 transs) of the photobleaching of Syx1a-EGFP. Three cells are in the image. Scale bar, $10 \mu m$. B) Recovery of Syx1a-EGFP (empty circles, N = 15 transmembrane circles, N = 15 transmembrane circles, N = 15 transmembrane proteins are in the image. Scale bar, N = 15 transmembrane circles, N = 15 transmembrane circles, N = 15 transmembrane proteins coated display and syx1a-GFP with Alexa594-NB* (pink circles, N = 15 transmembrane circles, N = 15 transmembrane proteins coated display and without the Alexa594-NB* (-NB). No statistically significant differences were observed between without NB and with labeled NB on fibronectin coated display. Standard error is shown in all plots. (For the interpretation of the reference to the color in this figure legend. The reader is referred to the web version of this article)

glass was treated in other ways to facilitate Fn coating. We used PLL first then adhered Fn. This led to slow and inconsistent movement of Alexa594-NB* labeled Syx1a-eGFP in FRAP experiments (Fig. S1). Increasing the concentration of Fn did not alleviate the slow motion (Fig. S1B). Therefore, this method was discontinued. Next, glass was cleaned by dipping in ethanol and flamed, followed by Fn coating. This method was simple to perform and did not impede motion of the Alexa594-NB* labeled Syx1a-eGFP in FRAP experiments (Fig. 4). The fraction mobile is the same with and without the Alexa594-NB* present (Fig. 4C). Qualitatively, cells also appeared more spread out on flame treated glass coated with Fn as opposed to KOH etched glass treated with Fn. This is observable by comparing representative cells shown in Figs. 3A and 4A.

Single Particle Tracking (SPT) methods show similar restrictions in dynamics with PLL coated surfaces. To determine if conclusions from FRAP experiments could be applied to other measurements of membrane protein dynamics, SPT experiments were performed on Alexa594-NB*. The NB* concentration was reduced 10-fold to facilitate tracking of single molecules. Molecules were imaged at 20 frames/second and then tracked. From the trajectories, the step size distributions and average step size for Alexa594-NB* on PLL and Fn over the course of 200 ms (4 frames) was measured (Fig. 5). The average step size for Alexa594-NB* attached to Syx1a-eGFP is approximately double for Fn coated surfaces compared to PLL (Fig. 5B). The histogram of the observed step sizes (Fig. 5A) shows a larger immobilized portion for PLL with a higher portion of small step sizes when compared to Fn.

To quantify the fraction of tracks that are immobile, Alexa594-NB* was immobilized by adhering to the surface of the PLL coated glass in the absence of cells. Immobilized NB* was tracked and the step size distribution was measured. All three distributions (immobilized, PLL and Fn) were fit to a two-component diffusion equation (Equation 1), to determine the rate of motion and portion of slow and fast tracks on each substrate. The slow component of the immobilized NB* (shown as a dotted line in Fig. 5A) was used to constrain the fit for Syx1a-EGFP labeled with Alexa594-NB* on PLL and Fn coated surfaces. From the fit of the step size distribution, the fraction of particles moving slowly was calculated; 17% of the tracks are immobile on Fn coated surfaces

and 36% of the tracks are immobile on PLL coated surfaces.

4. Discussion

One challenge for the accurate measurement of protein motion is that some membrane proteins are immobile due to pertinent biological interactions (*i.e.* clustering), whereas other membrane proteins, within the same cell, may be immobile due to issues with substrate interactions. Therefore, it is of utmost importance to reduce immobilization artifacts when measuring dynamics. In this work we describe a simple FRAP-based assay that allows for the specific characterization of the role of an organic dye on membrane protein motion by comparing the dynamics of Syx1a-GFP with a nanobody that has or doesn't have a red dye attached. We focus on a commonly used red fluorescent dye, Alexa594, and common surface coatings used for cell attachment.

To test for interactions that interfere with dynamic measurements, we used a differential, FRAP-based measurement, where the interference in protein diffusion due to the dye could be separately assessed relative to the interference due to the NB alone. The NB specifically binds transfected cells (Fig. 1) where a model transmembrane protein, Syx1a-EGFP, presents EGFP on the exterior surface. In the control lacking any NB, Syx1a-EGFP recovers at about 70% (Figs. 2B, 3B, 4B) on both Fn and PLL coated coverglass. This is in close agreement with others, where it is well established that Syx1a forms clusters on the surface of cells [19, 20, 27, 28, 30, 31] and these clusters are interchangeable with the surroundings [20, 28]. However, a portion (30-40%) of these molecules are immobile in FRAP measurements [28]. This recovery is increased when cytoplasmic domains of the protein that are known to interact with other molecules, such as the SNARE domain, are removed [28], suggesting that the immobile fraction is physiologically relevant.

Although cells adhere well to PLL coated coverglass, the dynamics of transmembrane proteins with dye labeled NB is inhibited. The Alexa594 dye on the NB hindered diffusion significantly more than the NB alone and the mobile fraction was reduced (Fig. 2) from 0.69 to 0.52 (Fig. 2B). Approximately ¼ of the mobile particles become immobile due to substrate interactions. This is not due to the NB alone because unlabeled NB

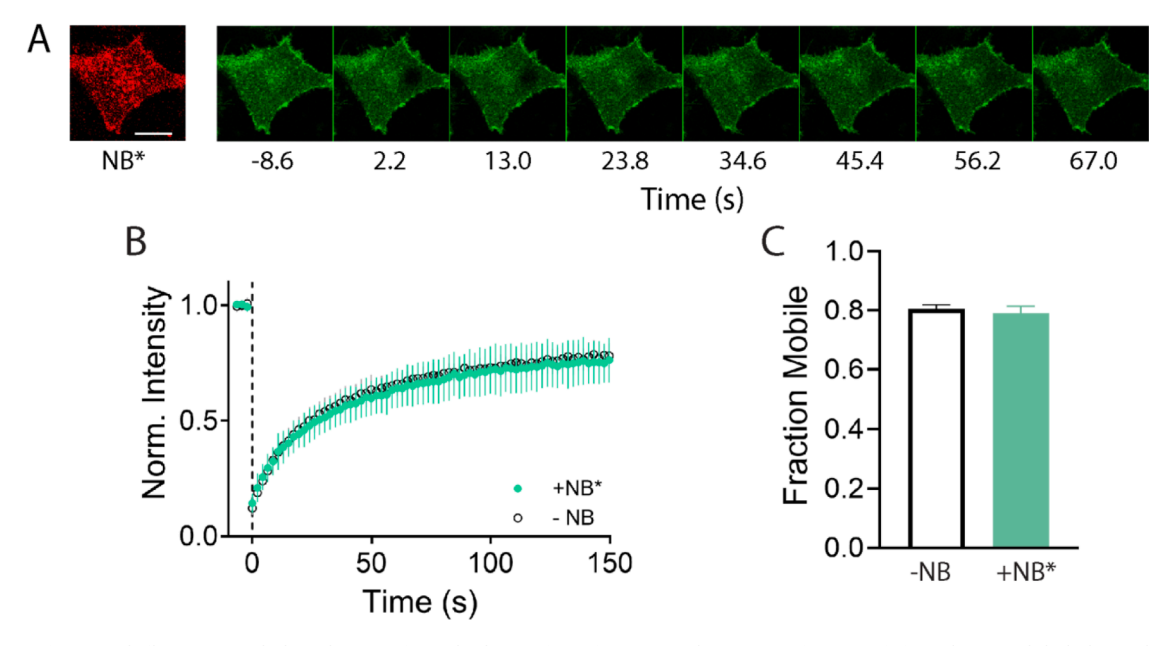


Fig. 4. Fibronectin-coated, flame-treated glass does not impede the motion of transmembrane proteins containing Alexa594 labeled nanobody. Glass was treated by dipping in ethanol and flamed then coated with fibronectin ($20 \,\mu\text{g/ml}$) and cells were plated then transiently transfected with Syx1a-EGFP. A) A confocal image of Alexa594-NB* (red) and a montage with images separated by 10.8 s (5 frames) of the photobleaching of Syx1a-EGFP. Scale bar, 10 $\,\mu\text{m}$. B) Recovery of Syx1a-EGFP (empty circles, N=20 cells) and Syx1a-EGFP with Alexa594-NB* (green circles, N=18 cells)), C) The fraction of Syx1a-EGFP that remains mobile with (NB*) and without the Alexa594-NB* (-NB). No statistically significant differences were observed between without NB and with labeled NB on Fn coated dishes. Standard error is shown in all plots. (For the interpretation of the reference to the color in this figure legend. The reader is referred to the web version of this article)

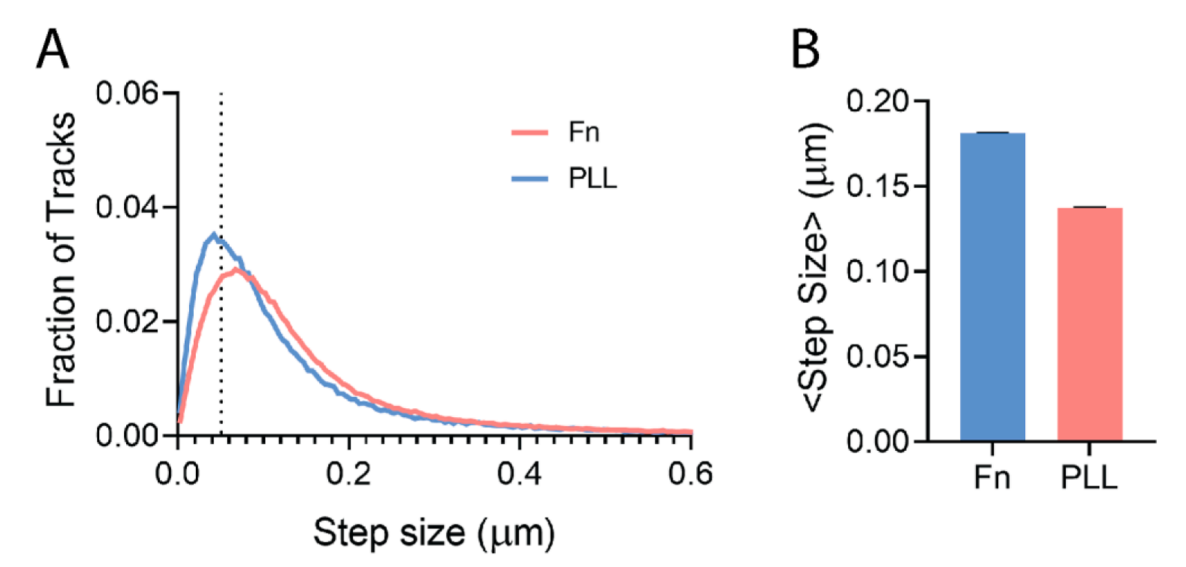


Fig. 5. Single molecule trajectories show reduced mobility on PLL relative to Fn. Single Alexa594-NB* molecules were tracked on the surface of Syx1a-EGFP containing PC12 cells using TIRF microscopy. A) The distribution of step sizes for Alexa594-NB* on cells expressing Syx1a-EGFP and grown on either PLL or Fn coated coverglass. The dotted line is the mean step size from fully immobile particles adhered to PLL coated coverglass in the absence of cells. The step size was measured over 200 ms. B) The average step size on different surface coatings. Error bars are SEM. (For the interpretation of the reference to the color in this figure legend. The reader is referred to the web version of this article)

does not show a decrease in mobility (Fig. 2). We hypothesized that the negatively charged dye interacts with the positively charged PLL surface coating, as suggested by others [13, 32]. Interactions have been observed previously for Congo Red, a negatively charged dye, and PLL via electrostatic interactions through two sulfonate groups. In this work, a change in the pH to 11 abolished the interaction [32], however this was not an option for cells in culture. Therefore, the surface coating was altered to test how protein dynamics are affected by the choice of glass coating for cell adhesion. Upon changing to Fn, protein mobility returned (Fig. 3) and the mobile fraction was restored. This demonstrates that the decrease in mobility on PLL is not due membrane interactions of the dye because the mobility is retained when the surface coating is changed to Fn. Therefore, this reduction in mobility is directly due to an interaction between the substrate and the dye, as others have suggested for different dyes and substrate combinations [13, 32].

Fibronectin came with challenges since it does not coat glass easily and several treatments of the glass were tested. Both KOH etched glass, which creates flat surfaces[18], and flame treated glass were easily coated with Fn and retained mobility in FRAP measurements (Figs. 3 and 4). However, when PLL was deposited prior to Fn to facilitate Fn adherence, dynamics were still hindered (Fig. S1A). This suggests that Fn may not fully cover the surface and additional Fn did not solve this issue (Fig. S1B).

To determine if the mobility measured by FRAP was translatable to other dynamic measurements, SPT was performed on cells containing Syx1a-EGFP and Alexa594-NB*. Note that in SPT measurements the red fluorescent NB channel was tracked and in FRAP data, the green fluorescent Syx1a-eGFP was measured. Based on the FRAP measurements, we expected that approximately 20-30% of spots observed in single molecule tracking should be confined or immobile (Figs. 2C, 3C and 4C) on Fn coated surfaces and approximately 50% should be immobile on PLL coated surfaces (Fig. 2C). Based on the step size distribution from single molecule trajectories, approximately 17% of tracks were immobile on Fn. This increased to 36% on PLL and SPT measurements appeared slightly more mobile than FRAP. The reason for the differences between the FRAP and SPT measurement of the immobile fraction is not entirely understood, but it is useful to note that the FRAP measurement measures the mobility over a larger distance with lower time resolution than SPT and often the rate of diffusion measured in SPT measurement is faster [33, 34]. In our work, the overall trend was the same; PLL immobilized the motion of transmembrane proteins significantly more than Fn.

Although mobility is an important factor for choosing substrates, Fn is also a natural choice for cell adherence. Fn is an extracellular matrix protein with binding sites that interact specifically with integrins, the glycoproteins responsible for cell binding and adhesion [16,17], whereas PLL relies on cell adhesion through electrostatic interactions. PLL has been used extensively for growing a wide variety of cells, including PC12 cells like those used here [19, 20] Fibronectin has also been used successfully with PC12 cells [17, 35-37]. However, other alternative coatings should be tested. Linearized PEG may be another good choice for a substrate coating with low interactions and no net charge [13] and a Tween20 based substrate coating may be another option for *in vitro* work requiring low substrate-dye interactions [38].

5. Conclusions

In conclusion, we recommend testing dyes with the substrates prior to cell dynamics measurements but demonstrate that Fn is a better choice than PLL for the Alexa594 dye tested here. Results here show that PLL is a poor choice of substrate for dynamics studies of transmembrane proteins with exogenous dye labeling (Fig. 2). However, Fn shows no inhibition of dynamics in FRAP based measurements (Fig. 3). Fn is easily coated onto glass that has been flame treated and cells readily attach (Fig. 4). Additionally, a novel, FRAP-based assay was designed to directly compare the dynamics of an EGFP-labeled membrane protein with and without the addition of a dye conjugated NB and this assay aligns well with single molecule tracking experiments (Fig. 5).

Declaration of Interests

The authors declare that they have no known competing financial interests or personal relationships that could have appeared to influence the work reported in this paper.

Acknowledgements

This research was supported by the National Science Foundation, Chemistry of Life Processes (NSF-CLP) program, project number 1807455.

Supplementary materials

Supplementary material associated with this article can be found, in the online version, at doi:10.1016/j.bbadva.2021.100026.

References

- [1] G. Giannone, E. Hosy, F. Levet, A. Constals, K. Schulze, A.I. Sobolevsky, M. P. Rosconi, E. Gouaux, R. Tampé, D. Choquet, L. Cognet, Dynamic superresolution imaging of endogenous proteins on living cells at ultra-high density, Biophys. J. 99 (2010) 1303–1310.
- [2] C.A. Buttler, N. Pezeshkian, M.V. Fernandez, J. Aaron, S. Norman, E.O. Freed, S. B. van Engelenburg, Single molecule fate of HIV-1 envelope reveals late-stage viral lattice incorporation, Nat. Commun. 9 (2018) 1861.
- [3] K. Lam, E. Tajkhorshid, Membrane Interactions of Cy3 and Cy5 Fluorophores and Their Effects on Membrane-Protein Dynamics, Biophys. J. 119 (2020) 24–34.
- [4] L.D. Lavis, Chemistry Is Dead. Long Live Chemistry!, Biochemistry 56 (2017) 5165–5170.
- [5] R.J. Rawle, A.M. Villamil Giraldo, S.G. Boxer, P.M. Kasson, Detecting and Controlling Dye Effects in Single-Virus Fusion Experiments, Biophys. J. 117 (2019) 445, 452
- [6] L.D. Hughes, R.J. Rawle, S.G. Boxer, Choose your label wisely: water-soluble fluorophores often interact with lipid bilayers, PLoS One 9 (2014) e87649.
- [7] N.C. Shaner, R.E. Campbell, P.A. Steinbach, B.N. Giepmans, A.E. Palmer, R. Y. Tsien, Improved monomeric red, orange and yellow fluorescent proteins derived from Discosoma sp. red fluorescent protein, Nat. Biotechnol. 22 (2004) 1567–1572.
- [8] D.M. Chudakov, M.V. Matz, S. Lukyanov, K.A. Lukyanov, Fluorescent proteins and their applications in imaging living cells and tissues, Physiol. Rev. 90 (2010) 1103–1163.
- [9] J.D. Knight, M.G. Lerner, J.G. Marcano-Velazquez, R.W. Pastor, J.J. Falke, Single molecule diffusion of membrane-bound proteins: window into lipid contacts and bilayer dynamics, Biophys. J. 99 (2010) 2879–2887.
- [10] T.W.M. De Groof, V. Bobkov, R. Heukers, M.J. Smit, Nanobodies: New avenues for imaging, stabilizing and modulating GPCRs, Mol. Cell. Endocrinol. 484 (2019) 15, 24
- [11] R. Kasula, Y.J. Chai, A.T. Bademosi, C.B. Harper, R.S. Gormal, I.C. Morrow, E. Hosy, B.M. Collins, D. Choquet, A. Papadopulos, F.A. Meunier, The Munc18-1 domain 3a hinge-loop controls syntaxin-1A nanodomain assembly and engagement with the SNARE complex during secretory vesicle priming, J. Cell Biol. 214 (2016) 847–858.
- [12] K.J. Seitz, S.O. Rizzoli, GFP nanobodies reveal recently-exocytosed pHluorin molecules, Sci. Rep. 9 (2019) 7773.
- [13] L.C. Zanetti-Domingues, M.L. Martin-Fernandez, S.R. Needham, D.J. Rolfe, D. T. Clarke, A systematic investigation of differential effects of cell culture substrates on the extent of artifacts in single-molecule tracking, PLoS One 7 (2012) e45655.
- [14] L.C. Zanetti-Domingues, C.J. Tynan, D.J. Rolfe, D.T. Clarke, M. Martin-Fernandez, Hydrophobic fluorescent probes introduce artifacts into single molecule tracking experiments due to non-specific binding, PLoS One 8 (2013) e74200.
- [15] A. Orlowska, P.T. Perera, M. Al Kobaisi, A. Dias, H.K.D. Nguyen, S. Ghanaati, V. Baulin, R.J. Crawford, E.P. Ivanova, The Effect of Coatings and Nerve Growth Factor on Attachment and Differentiation of Pheochromocytoma Cells, Materials (Basel) 11 (2017).
- [16] H. Bachman, J. Nicosia, M. Dysart, T.H. Barker, Utilizing Fibronectin Integrin-Binding Specificity to Control Cellular Responses, Adv Wound Care (New Rochelle) 4 (2015) 501–511.
- [17] K.J. Tomaselli, C.H. Damsky, L.F. Reichardt, Interactions of a neuronal cell line (PC12) with laminin, collagen IV, and fibronectin: identification of integrin-related glycoproteins involved in attachment and process outgrowth, J. Cell Biol. 105 (1987) 2347–2358.

- [18] N. Chada, K.P. Sigdel, R.R.S. Gari, T.R. Matin, L.L. Randall, G.M. King, Glass is a Viable Substrate for Precision Force Microscopy of Membrane Proteins, Sci. Rep. 5 (2015) 12550.
- [19] M.K. Knowles, S. Barg, L. Wan, M. Midorikawa, X. Chen, W. Almers, Single secretory granules of live cells recruit syntaxin-1 and synaptosomal associated protein 25 (SNAP-25) in large copy numbers, Proc. Natl. Acad. Sci. USA 107 (2010) 20810–20815.
- [20] S. Barg, M.K. Knowles, X. Chen, M. Midorikawa, W. Almers, Syntaxin clusters assemble reversibly at sites of secretory granules in live cells, Proc. Natl. Acad. Sci. USA 107 (2010) 20804–20809.
- [21] J.C. Black, P.P. Cheney, T. Campbell, M.K. Knowles, Membrane Curvature Based Lipid Sorting Using a Nanoparticle Patterned Substrate, Soft Matter 10 (2014) 2016–2023
- [22] P.P. Cheney, M.D. Stachler, M.K. Knowles, Single Molecule Tracking of P-glycoprotein in Live Cells Reveals Dynamic Heterogeneity, in: 34th Annual International Conference of the IEEE EMBS, 2012, pp. 3159–3162.
- [23] P.P. Cheney, A.W. Weisgerber, A.M. Feuerbach, M.K. Knowles, Single Lipid Molecule Dynamics on Supported Lipid Bilayers with Membrane Curvature, Membranes 7 (2017).
- [24] D. Blair, Dufresne, E., The Matlab Particle Tracking Code Repository, https://site. physics.georgetown.edu/matlab/, accessed 2014.
- [25] J.C. Crocker, D.G. Grier, Methods of Digital Video Microscopy for Colloidal Studies, J. Colloid Interface Sci. 179 (1996) 298.
- [26] T. Lang, D. Bruns, D. Wenzel, D. Riedel, P. Holroyd, C. Thiele, R. Jahn, SNAREs are concentrated in cholesterol-dependent clusters that define docking and fusion sites for exocytosis, EMBO J. 20 (2001) 2202–2213.
- [27] J.J. Sieber, K.I. Willig, R. Heintzmann, S.W. Hell, T. Lang, The SNARE motif is essential for the formation of syntaxin clusters in the plasma membrane, Biophys. J. 90 (2006) 2843–2851.
- [28] J.J. Sieber, K.I. Willig, C. Kutzner, C. Gerding-Reimers, B. Harke, G. Donnert, B. Rammner, C. Eggeling, S.W. Hell, H. Grubmuller, T. Lang, Anatomy and dynamics of a supramolecular membrane protein cluster, Science 317 (2007) 1072–1076.
- [29] N.R. Gandasi, S. Barg, Contact-induced clustering of syntaxin and munc18 docks secretory granules at the exocytosis site, Nat. Commun. 5 (2014) 3914.
- [30] T. Lang, D. Bruns, D. Wenzel, D. Riedel, P. Holroyd, C. Thiele, R. Jahn, SNAREs are concentrated in cholesterol-dependent clusters that define docking and fusion sites for exocytosis, EMBO J. 20 (2001) 2202–2213.
- [31] S. Sharma, M. Lindau, t-SNARE Transmembrane Domain Clustering Modulates Lipid Organization and Membrane Curvature, J. Am. Chem. Soc. 139 (2017) 18440–18443.
- [32] E. Pigorsch, A. Elhaddaoui, S. Turrell, Studies of the binding mechanism of Congo red to poly(L-lysine) by absorption and circular dichroism spectroscopy, J. Mol. Struct. 348 (1995) 61–64.
- [33] L. Guo, J.Y. Har, J. Sankaran, Y. Hong, B. Kannan, T. Wohland, Molecular Diffusion Measurement in Lipid Bilayers over Wide Concentration Ranges: A Comparative Study, ChemPhysChem 9 (2008) 721–728.
- [34] M.I.E. Harwardt, M.S. Dietz, M. Heilemann, T. Wohland, SPT and Imaging FCS Provide Complementary Information on the Dynamics of Plasma Membrane Molecules, Biophys. J. 114 (2018) 2432–2443.
- [35] R. Akeson, S.L. Warren, PC12 adhesion and neurite formation on selected substrates are inhibited by some glycosaminoglycans and a fibronectin-derived tetrapeptide, Exp. Cell Res. 162 (1986) 347–362.
- [36] S. Johansson, L. Kjellén, M. Höök, R. Timpl, Substrate adhesion of rat hepatocytes: a comparison of laminin and fibronectin as attachment proteins, J. Cell Biol. 90 (1981) 260–264
- [37] A. Orlowska, P.T. Perera, M. Al Kobaisi, A. Dias, H.K.D. Nguyen, S. Ghanaati, V. Baulin, R.J. Crawford, E.P. Ivanova, The Effect of Coatings and Nerve Growth Factor on Attachment and Differentiation of Pheochromocytoma Cells, Materials (Basel) 11 (2017) 60.
- [38] B. Hua, K.Y. Han, R. Zhou, H. Kim, X. Shi, S.C. Abeysirigunawardena, A. Jain, D. Singh, V. Aggarwal, S.A. Woodson, T. Ha, An improved surface passivation method for single-molecule studies, Nat. Methods 11 (2014) 1233–1236.